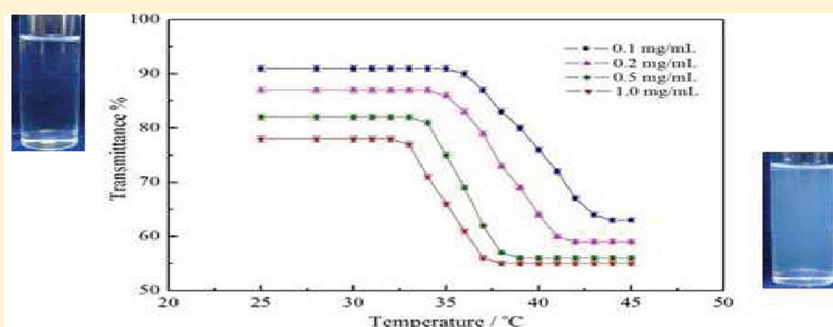


Synthesis and Self-Assembly of Thermoresponsive PEG-*b*-PNIPAM-*b*-PCL ABC Triblock Copolymer through the Combination of Atom Transfer Radical Polymerization, Ring-Opening Polymerization, and Click Chemistry

Jiucun Chen, Mingzhu Liu,* Honghong Gong, Yinjuan Huang, and Chen Chen

State Key Laboratory of Applied Organic Chemistry, Key Laboratory of Nonferrous Metal Chemistry and Resources Utilization of Gansu Province, and Department of Chemistry, Lanzhou University, Lanzhou 730000, People's Republic of China

ABSTRACT:



A well-defined thermoresponsive poly(ethylene glycol)-*block*-poly(*N*-isopropylacrylamide)-*block*-poly(ϵ -caprolactone) (PEG₄₃-*b*-PNIPAM₈₂-*b*-PCL₈₇) triblock copolymer was synthesized by combination of atom transfer radical polymerization (ATRP), ring-opening polymerization (ROP), and click chemistry. The synthesis included the four steps, and all the structures of the polymers were determined. The thermoresponsive triblock copolymer can disperse in water at room temperature to form core–shell–corona micelles with the hydrophobic PCL block as core, the thermoresponsive PNIPAM block as shell, and the hydrophilic PEG block as corona. At temperatures above the lower critical solution temperature (LCST) of the PNIPAM block, the PNIPAM chains gradually collapse on the PCL core to shrink the size and change the structure of the resultant core–shell–corona micelles with temperature increasing.

INTRODUCTION

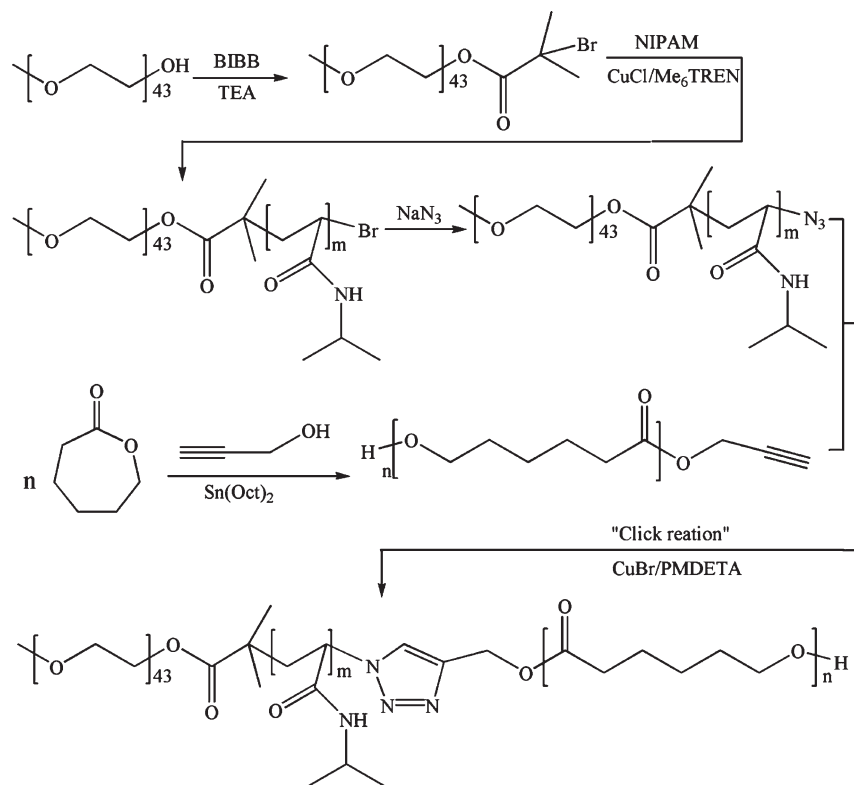
Amphiphilic copolymers composed of hydrophilic and hydrophobic segments can assemble into core–shell micelles in aqueous media that have a compact core formed by the insoluble segments and a stretched shell formed by the soluble segments. They have potential applications as drug carriers for controlled-release.^{1–3} For example, various morphological core–shell micelles are self-assembled by amphiphilic diblock copolymers such as poly(glycidyl methacrylate)-*block*-poly(poly(ethylene glycol)-methyl ether methacrylate),⁴ poly(*tert*-butyl acrylate)-*block*-poly(glycidyl methacrylate).⁵ Choosing some stimuli-responsive polymers can make the core–shell micelles responsive to pH and temperatures, such as poly(*t*-butyl acrylate-*co*-acrylic acid)-*b*-poly(*N*-isopropylacrylamide)⁶ and polystyrene-*b*-poly(*N*-isopropylacrylamide).⁷ Besides core–shell micelles, other types of three-layered micelles such as “onion-type” micelles and core–shell–corona micelles have also been studied. These three-layered micelles may provide innovative applications and understanding of the structure and dynamics of micelles and also may influence general concepts about polymer stabilization of colloids and the self-assembly of polymers.^{8,9} Compared with core–shell

micelles, core–shell–corona micelles are scarcely studied,¹⁰ which is possibly due to the difficulty in synthesis of the triblock copolymers and partly due to the complicated structure of three-layered micelles. Up to date, several routes can be considered to synthesize block copolymers. The most convenient consists in the successive polymerization of two or more monomers without purification steps of intermediate compounds.¹¹ However, this method is strongly limited to a few monomers, usually with the same chemical and physical properties (i.e., similar radical reactivity), which make them often inadequate for the material synthesis by self-assembly. An alternative route is the so-called macroinitiator method:¹² a polymer chain is chemically modified to be end-functionalized by an initiator molecule in order to trigger the polymerization of the second or third monomer. Although this method is applicable to a large variety of monomers, the presence of residual homopolymers potentially hidden by an increase of the molar mass distribution is difficult to avoid,

Received: September 2, 2011

Revised: November 10, 2011

Published: November 14, 2011

Scheme 1. Schematic Illustration of the Synthesis of Triblock Copolymer of PEG-*b*-PNIPAM-*b*-PCL

three-neck flask. After azeotropic distillation of about 60 mL toluene at reduced pressure to remove traces of water, 2.5 mL of TEA was added and the mixed solution was cooled to 0 °C. Then 2.0 mL of 2-bromoisobutyl bromide was added dropwise via syringe over 1 h, and the reaction mixture was stirred overnight at room temperature. Most of the toluene was removed by rotary evaporation prior to precipitation into a 10-fold excess of cold ether. The crude polymer was dried under vacuum, dissolved in water at pH 8–9, and then extracted with CH₂Cl₂. The organic layers were collected and dried over MgSO₄, and removal of the solvent under vacuum led to isolation of the purified macro-initiator (PEG₄₃-Br).

Synthesis of Tris(2-(dimethylamino)ethyl)amine (Me₆TREN). Tris(2-dimethylaminoethyl)amine (Me₆TREN) was prepared according to the previous report.³² A mixture of 1.8 g of tris(2-aminoethyl)amine, 1.5 mL of water, 10 mL of 85% formic acid, and 9 mL of 30% formaldehyde was introduced into a 100 mL round-bottom flask and heated at 120 °C until no carbon dioxide was produced. All the volatile fractions were then removed by vacuum distillation. The solid residue was then added to 100 mL of 10 wt % NaOH aqueous solution; an oily layer formed which was extracted with Et₂O. The Et₂O extract was dried over potassium hydroxide for 12 h. After removal of the Et₂O, a colorless oil compound was obtained. Yield = 65%. ¹H NMR (CDCl₃, ppm): 2.21 (s, 18H, ((CH₃)₂N-CH₂-CH₂)₃N), 2.35–2.38 (t, 6H, ((CH₃)₂N-CH-CH₂)₃N), 2.57–2.61 (t, 6H, ((CH₃)₂N-CH₂-CH₂)₃N).

Synthesis of PEG₄₃-*b*-PNIPAM₈₂. PEG₄₃-*b*-PNIPAM₈₂ was synthesized by ATRP using the haloid-tailed PEG₄₃-Br as the macroinitiator. An amount of 2.3 g (0.885 mmol) of PEG₄₃-Br was added into a reaction flask, and then 30 mL of solvent

mixture of butanone and 2-propanol (1:1 by volume) was added. The sample was first stirred and then degassed under nitrogen purge. Subsequently, 0.0876 g (0.885 mmol) of CuCl and 0.204 g (0.885 mmol) of Me₆TREN were introduced into the reaction flask. At last, 10.0 g (88.5 mmol) of NIPAM was added into the flask, and the mixture was degassed under nitrogen purge. Polymerization was performed at 60 °C for 4 h, and NIPAM conversion was 49%. The resultant solution was first evaporated to dryness under vacuum. The residue was diluted with THF and passed through an alumina column to remove the copper catalyst. The product was precipitated from ether three times and then dried under vacuum overnight at room temperature to produce the block copolymer PEG₄₃-*b*-PNIPAM₈₂ as a white powder.

General Procedure for the Synthesis of PEG₄₃-*b*-PNIPAM₈₂-N₃. Amounts of 2.0 g (0.168 mmol) of PEG₄₃-*b*-PNIPAM₈₂ and 0.0218 g (0.335 mmol) of NaN₃ were dissolved in 20 mL of DMF, and the reaction mixtures were stirred for 24 h at room temperature. Purification of the product was done by precipitation into a 10-fold excess of cold ether. The precipitated polymer was filtered off and washed with cold ether. This precipitation procedure was done twice. Finally the PEG₄₃-*b*-PNIPAM₈₂-N₃ was dried at room temperature under vacuum.

Synthesis of Propargyl-Terminated PCL by ROP. The propargyl-terminated PCL was prepared by ROP of ε-CL in toluene with Sn(Oct)₂ as a catalyst and propargyl alcohol as an initiator as the reported procedure.³³ In a typical procedure, propargyl alcohol (0.053 g, 0.95 mmol) and ε-CL (12 g, 105 mmol) were added to freshly dried toluene (50 mL) in a flask, and then Sn(Oct)₂ (0.194 g, 0.48 mmol) was added and the flask was then placed in a thermostatted oil bath at 100 °C for 4 h. After the polymerization, the mixture was cooled to room temperature,

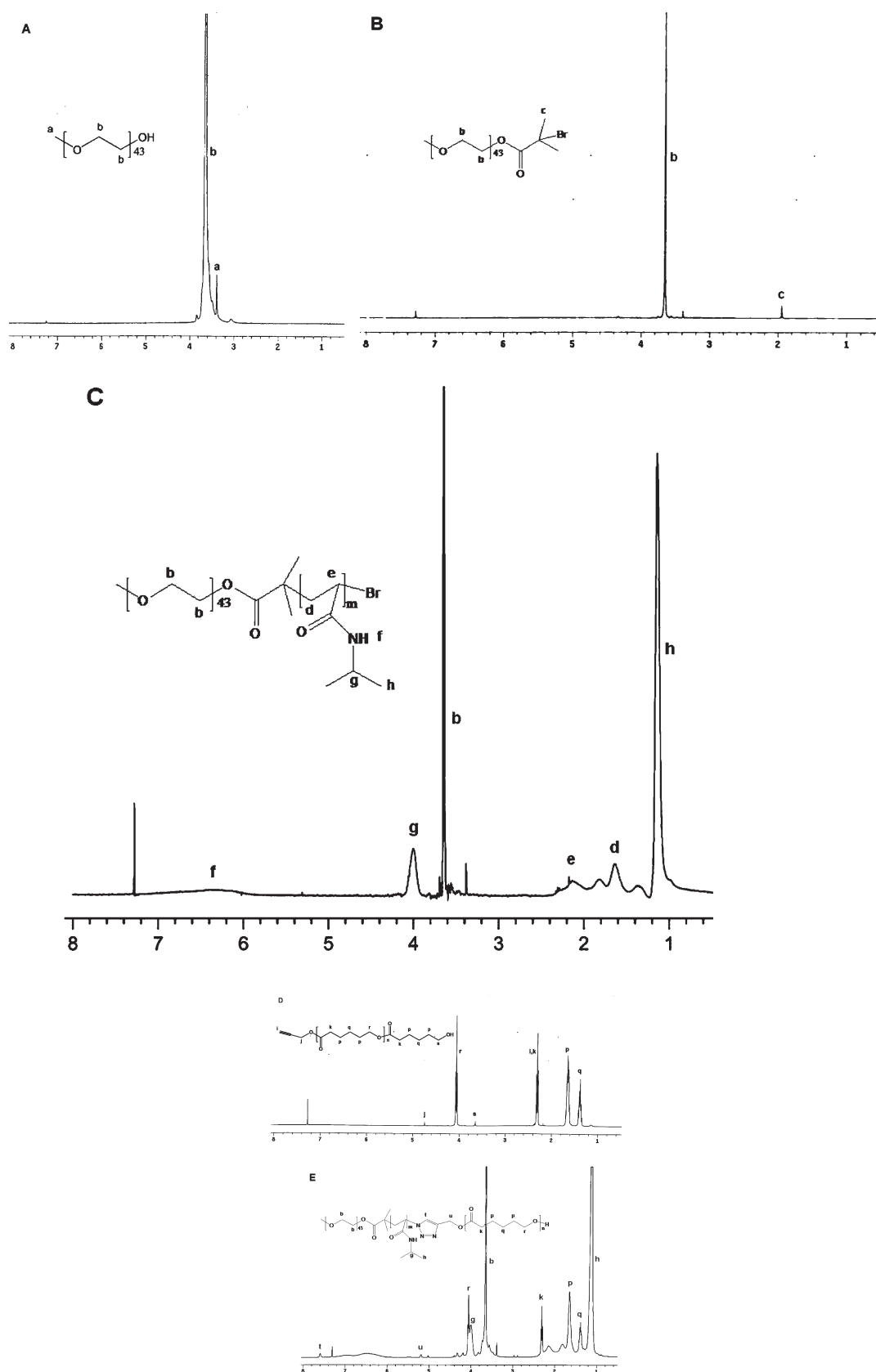


Figure 1. ^1H NMR spectra and peak labels for (A) PEG_{43} , (B) $\text{PEG}_{43}\text{-Br}$, (C) $\text{PEG}_{43}\text{-}b\text{-PNIPAM}_{82}$, (D) the propargyl-terminated PCL_{87} , and (E) $\text{PEG}_{43}\text{-}b\text{-PNIPAM}_{82}\text{-}b\text{-PCL}_{87}$ (in CDCl_3 , ppm).

precipitated into an excess amount of cold ether, filtered off, and dried at room temperature in a vacuum oven for 24 h ($M_n = 9300$, $M_w/M_n = 1.09$). Other propargyl-terminated PCLs (PCL₂₈ and PCL₅₀) were prepared with a similar method.

Synthesis of PEG₄₃-*b*-PNIPAM₈₂-*b*-PCL₈₇ through Click Reaction: A General Procedure. The general procedure for the click reaction was as follows: in a flask equipped with a magnetic stirring bar, 1.416 g (0.12 mmol) of PEG₄₃-*b*-PNIPAM₈₂-N₃, 0.93 g (0.10 mmol) of propargyl-terminated PCL₈₇, 0.0143 g (0.10 mmol) of CuBr, and THF (10 mL) were added. The flask was capped with a rubber plug and purged with N₂ for 15 min. An amount of 0.0173 g (0.10 mmol) of PMDETA was then added by using a degassed syringe. After stirring for 24 h at room temperature, the mixture was passed through a short Al₂O₃ column to remove the copper complex, and the solution was dialyzed against deionized water using a dialysis membrane (cutoff molecular weight: 14 000) for 48 h and subsequently lyophilized in a Labconco freeze drier (Freezone 2.5 liter, model 7670530) for 12 h.

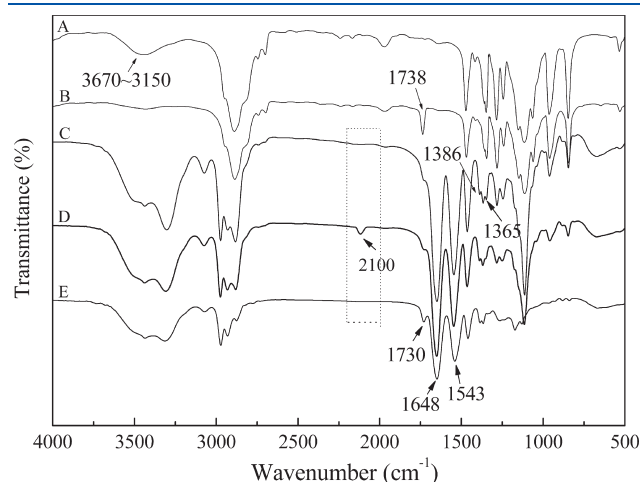


Figure 2. FTIR spectra obtained for (A) PEG₄₃, (B) PEG₄₃-Br, (C) PEG₄₃-*b*-PNIPAM₈₂, (D) PEG₄₃-*b*-PNIPAM₈₂-N₃, and (E) PEG₄₃-*b*-PNIPAM₈₂-*b*-PCL₈₇.

RESULTS AND DISCUSSION

The overall experiment is illustrated in Scheme 1. In this study, the precursors PEG-*b*-PNIPAM-Br are first prepared by ATRP of *N*-isopropylacrylamide initiated with a PEO-Br macroinitiator, which is obtained from the esterification of 2-bromoisobutyryl bromide and CH₃O-PEG-OH. The functionality transformation is then performed by a substitution reaction to generate the azido-terminated precursor PEG-*b*-PNIPAM-N₃. The propargyl-terminated PCL was prepared by the ROP of ϵ -caprolactone initiated with propargyl alcohol in the presence of stannous octanoate. The novel triblock copolymers PEG-*b*-PNIPAM-*b*-PCL are synthesized by a click reaction of PEG-*b*-PNIPAM-N₃ and propargyl-terminated PCL in the presence of a CuBr/PMDETA catalyst system.

Figure 1A shows the ¹H NMR spectrum of CH₃O-PEG₄₃-OH. The ¹H NMR spectrum of the PEG₄₃-Br macroinitiator is shown in Figure 1B. The chemical shift at $\delta = 1.92$ ppm was associated with the methyl protons (c, C(Br)-CH₃) of the 2-bromoisobutyryl groups.³⁴ The chemical shift at $\delta = 3.63$ ppm was attributable to the inner methylene protons adjacent to the oxygen moieties (b, O-CH₂). From the area of peaks c and a as shown in the ¹H NMR spectrum of Figure 1B, it can be concluded that all CH₃O-PEG₄₃-OH has been transformed into PEG₄₃-Br. Figure 2, parts A and B, reveals the representative FTIR spectra of PEG₄₃ and PEG₄₃-Br. The conversion of PEG₄₃ to PEG₄₃-Br was confirmed by the almost disappearance of -OH stretching at 3670–3150 cm⁻¹ of PEG₄₃ in the FTIR spectrum, while the peak at 1738 cm⁻¹ was assigned to the carbonyl stretching vibration of the ester group. PEG₄₃-*b*-PNIPAM₈₂ diblock copolymer was synthesized by the ATRP polymerization of NIPAM using PEG₄₃-Br as the macroinitiator, and its ¹H NMR spectrum is shown in Figure 1C. Besides the characteristic peaks of PEG residues, characteristic signals of PNIPAM at $\delta = 4.0$ (g) and 1.1 (h) ppm representing methyne and methyl protons on isopropyl groups were observed, which verified the successful synthesis of diblock copolymer. The average DP_n of PNIPAM blocks was obtained based on the area ratio of peak g to peak b. FTIR also confirmed that PEG₄₃-*b*-PNIPAM₈₂ was

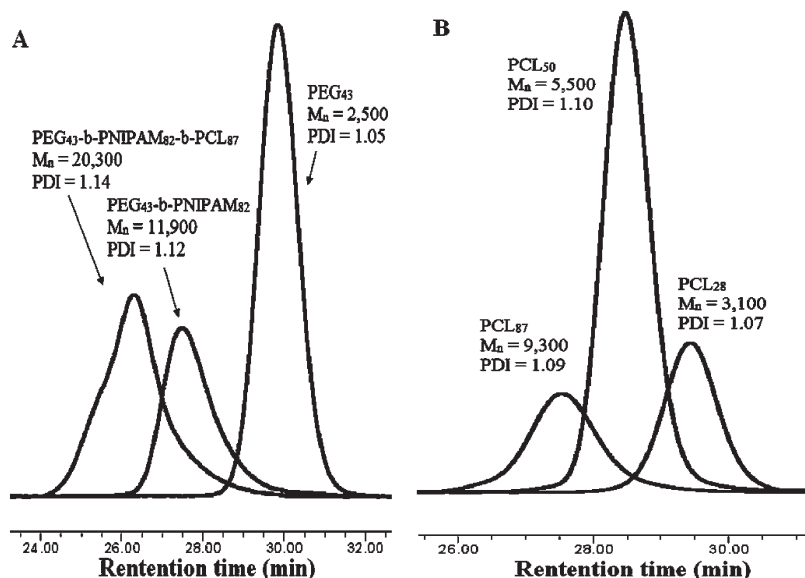


Figure 3. GPC traces of (A) PEG₄₃, PEG₄₃-*b*-PNIPAM₈₂, PEG₄₃-*b*-PNIPAM₈₂-PCL₈₇, and (B) PCL₂₈, PCL₅₀, PCL₈₇.

Table 1. Characterization of Polymers

polymer	$[M]_0/[I]_0$	time (h)	$M_{n,NMR}$ (kDa) ^a	DP_{NMR} ^a	$M_{n,GPC}$ (kDa) ^b	M_w/M_n ^b
PEG ₄₃			1.9	45 (PEG)	2.5	1.05
PEG ₄₃ –Br			2.0	45 (PEG)	2.6	1.05
PEG ₄₃ - <i>b</i> -PNIPAM ₄₉	100 ^c	1	7.5	49 (PNIPAM)	7.8	1.07
PEG ₄₃ - <i>b</i> -PNIPAM ₆₈	100 ^c	2	9.7	68 (PNIPAM)	9.6	1.08
PEG ₄₃ - <i>b</i> -PNIPAM ₈₂	100 ^c	4	11.3	82 (PNIPAM)	11.9	1.12
PEG ₄₃ - <i>b</i> -PNIPAM ₈₂ –N ₃			11.3	82 (PNIPAM)	11.8	1.11
PCL ₂₈	40 ^d	4	3.2	28 (PCL)	3.1	1.07
PCL ₅₀	70 ^d	4	5.7	50 (PCL)	5.5	1.10
PCL ₈₇	110 ^d	4	9.9	87 (PCL)	9.3	1.09
PEG ₄₃ - <i>b</i> -PNIPAM ₈₂ - <i>b</i> -PCL ₈₇			23.7	87 (PCL)	20.3	1.14

^a Calculated on the basis of ¹H NMR results. ^b Determined by GPC. ^c $[M]_0/[I]_0$ is the molar ratio of [NIPAM]₀/[PEG₄₃–Br]₀. ^d $[M]_0$ and $[I]_0$ are the initial concentrations of ϵ -CL and propargyl alcohol, respectively.

successfully prepared. Compared to the FTIR spectrum of PEG₄₃–Br, we can clearly observe the amide I band (1648 cm^{−1}, C=O stretching) and amide II band (1543 cm^{−1}, N–H stretching) (Figure 2C). The presence of two bands at 1365 and 1386 cm^{−1} are associated with the deformation of two methyl groups on isopropyl.³⁵ According to GPC results the apparent molecular weight (M_n) and the polydispersity (M_w/M_n) of PEG₄₃-*b*-PNIPAM₈₂ are 11 900 and 1.12, respectively (Figure 3A).

Xia et al.³⁶ showed that ATRP of NIPAM in different alcohols, especially in 2-propanol, that alleviate catalyst inactivation by hydrogen bonding between amide groups and branched alcohols, led to narrow-disperse PNIPAM with high conversion and good molecular weight control. Me₆TREN, a branched tetradentate ligand, forms one of the most active catalyst complexes among all the ligands that have been investigated, with particular success in ATRP of acrylamides with good control over polymerization in room temperature.³⁷ Tu et al.³⁸ investigated the polymerization of NIPAM under a range of reaction conditions to investigate the catalysts and reaction temperature effect on ATRP. They found that the reaction catalyzed by CuBr at 20 °C gave the fastest polymerization rate, and the kinetic plot is nonlinear. This highly active CuBr/Me₆TREN has a large equilibrium constant in the ATRP and can rapidly drive the initiators to generate high radical concentration at early stages of polymerization. In order to alleviate the fast polymerization rate, the halide exchange (R–Br/Cu(I)Cl) catalyst system with Me₆TREN as ligand was performed. In this study, the bromo-terminated PEG-*b*-PNIPAM of low molecular weight was synthesized through ATRP using CuCl/Me₆TREN as the catalyst and PEG₄₃–Br as the macro-initiator. The ATRP reactions were stopped at relatively low monomer conversions to ensure a high degree of bromine end-functionality.^{19,39,40} The ATRP polymerization of NIPAM was carried out in mixed solvent using PEG₄₃–Br as the macro-initiator and thermal initiation at 60 °C with molar ratio of [NIPAM]/[PEG₄₃–Br] = 100:1. Detailed experimental conditions and results are listed in Table 1. In order to ensure a high degree of terminal bromine functionality, the monomer conversion was controlled to less than 50%. After the polymerization period of 1, 2, and 4 h, PEG₄₃-*b*-PNIPAM₄₉, PEG₄₃-*b*-PNIPAM₆₈, and PEG₄₃-*b*-PNIPAM₈₂ were obtained with monomer conversions of 27%, 36%, and 49%, respectively.

Subsequently, the terminal bromine of PEG₄₃-*b*-PNIPAM₈₂ was transformed into an azide group by simple nucleophilic substitution reactions in DMF in the presence of an excess of

NaN₃. The FTIR spectra of PEG₄₃-*b*-PNIPAM₈₂–N₃ clearly reveals the new appearance of an absorbance peak around 2100 cm^{−1} (Figure 2D), which is characteristic of a terminal azido group.^{41,42} By GPC analysis, the synthesis of the PEG₄₃-*b*-PNIPAM₈₂–N₃ precursors involved no molecular weight reduction, based on the observation of narrow symmetrical signals present at the same position as the starting PEG₄₃-*b*-PNIPAM₈₂–Br precursors.

The controlled ring-opening polymerization (CROP) of ϵ -CL monomer was performed in the presence of the catalyst, Sn(Oct)₂, and an initiator, propargyl alcohol, in toluene at 100 °C. Three different monomer/initiator ratios were utilized to obtain controlled propargyl-terminated PCLs and achieve different molecular weights (Figure 3B). Detailed information is listed in Table 1. The structural characteristics of the obtained linear PCL₈₂ have been determined by ¹H NMR analysis in Figure 1D. The resonance at 4.71 ppm (j) was the characteristic signal of the methylene protons of propargyl group, while resonance of the alkynyl proton (i) was overlapped with that of methylene protons of PCL₈₂ at 2.33 ppm (k). The triplet at 3.64 ppm (s) was assigned to the PCL₈₂ methylene protons conjoint with the hydroxyl end group. The degree of polymerization (DP) of PCLs can be calculated by the integration ratio of signals at 4.05 ppm (r) of the PCLs repeat units and that of signal at 3.64 ppm (s). This verifies that the ROP of ϵ -CL is successful. Furthermore, by GPC analysis, the PCL precursor had a low polydispersity index (Table 1). So, the propargyl-terminated PCL can be prepared by the ROP of ϵ -CL initiated with propargyl alcohol and in the presence of the catalyst Sn(Oct)₂.

Finally, using a click reaction, the azide end groups of PEG₄₃-*b*-PNIPAM₈₂ and the propargyl-terminated PCL₈₇ were reacted to give the corresponding PEG₄₃-*b*-PNIPAM₈₂-*b*-PCL₈₇ in the presence of a CuBr/PMDETA catalyst system in THF at room temperature. To make the click reaction completely, excess of the PEG₄₃-*b*-PNIPAM₈₂–N₃ was used. After click reaction, unreacted PEG₄₃-*b*-PNIPAM₈₂–N₃ was removed successfully using dialysis. In the ¹H NMR spectrum shown in Figure 1E, all of the protons of the PEG₄₃-*b*-PNIPAM₈₂ and PCL₈₅ segments can be assigned. More importantly, resonances at 7.60 ppm (t) and 5.20 ppm (u) are obvious, which should be assigned to the protons of the 1,2,3-triazole ring and the methylene protons of PCL conjoint to the 1,2,3-triazole ring, and this demonstrated the successful performance of the click reaction. As shown in Figure 2E, comparing to PEG₄₃-*b*-PNIPAM₈₂–N₃, the peak at

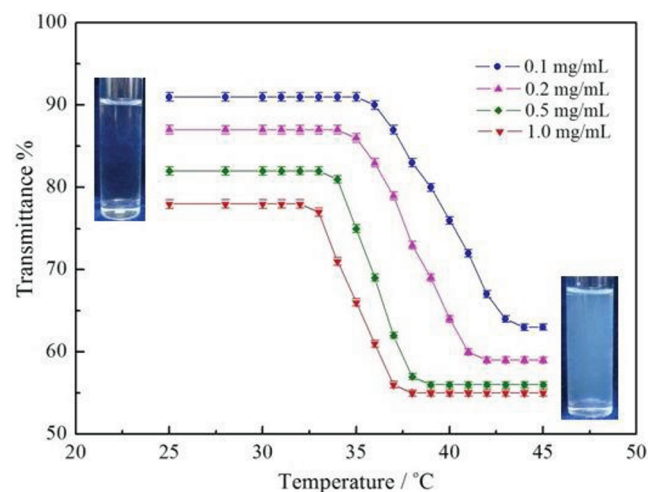


Figure 4. Temperature dependences of optical transmittance at 500 nm obtained for aqueous solutions of PEG₄₃-*b*-PNIPAM₈₂-*b*-PCL₈₇ at varying polymer concentrations.

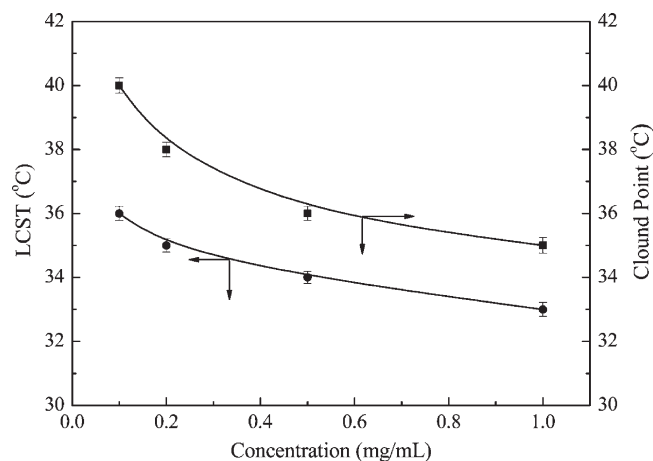


Figure 5. Concentration dependences of LCSTs and CPs obtained for aqueous solutions of PEG₄₃-*b*-PNIPAM₈₂-*b*-PCL₈₇. LCST and CP values were defined as the temperatures corresponding to 1% and 50% decreases of transmittance, respectively.

2100 cm^{-1} from N_3 disappeared completely while the peak at 1730 cm^{-1} from $\text{C}=\text{O}$ groups appeared in the IR curve of PEG₄₃-*b*-PNIPAM₈₂-*b*-PCL₈₇, indicating that the cycloaddition reaction was successful. From the GPC profiles in Figure 3A, we clearly observed that GPC chromatography of PEG₄₃-*b*-PNIPAM₈₂-*b*-PCL₈₇ shifts toward high molecular weight direction as compared to that of PEG₄₃-*b*-PNIPAM₈₂ diblock polymer and PCL₈₇, while neither PEG₄₃-*b*-PNIPAM₈₂- N_3 nor PCL₈₇ traces were found. This suggests that click coupling is complete. In addition, by comparing the integral of signals b and k in the ^1H NMR spectrum shown in Figure 1E, the ratio of protons is in agreement with the theoretical value, verifying the unique existence of PEG₄₃-*b*-PNIPAM₈₂-*b*-PCL₈₇ triblock copolymer. All of the results confirm that PEG₄₃-*b*-PNIPAM₈₂-*b*-PCL₈₇ was successfully prepared.

Thermal phase transition temperature, expressed as lower critical solutions temperature (LCST) and/or cloud point (CP), is one of the basic physical properties of thermoresponsive

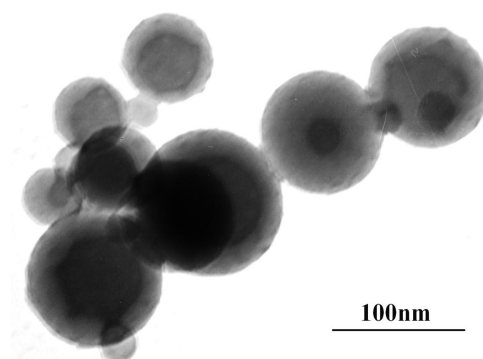


Figure 6. TEM images of micelles formed by PEG₄₃-*b*-PNIPAM₈₂-*b*-PCL₈₇ triblock copolymer.

water-soluble polymers. Temperature-dependent turbidimetry was then employed to determine LCST and CP values of PEG₄₃-*b*-PNIPAM₈₂-*b*-PCL₈₇ micelles in aqueous solutions. It should be noted that CP is a macroscopic parameter defining the temperature at which the solution turns turbid, which can also be checked by visual inspection. On the other hand, LCST is a thermodynamic parameter defining the critical temperature at which interchain aggregation starts to occur. For convenience and direct comparison to the results obtained by Qiu et al.,⁴³ in subsequent sections, LCST and CP values were defined as the temperature at which 1% and 50% decreases of transmittance could be observed, respectively. Figure 4 shows the temperature-dependent transmittance at a wavelength of 500 nm obtained for aqueous solutions of PEG₄₃-*b*-PNIPAM₈₂-*b*-PCL₈₇ micelles at different concentrations. In both cases, we can clearly see that both LCST and CP values increase with decreasing the triblock copolymer concentrations and that the lower the polymer concentration is, the broader is the temperature range exhibiting the decrease of transmittance. Thus, the relative magnitude of CP values of PEG₄₃-*b*-PNIPAM₈₂-*b*-PCL₈₇ strongly depends upon polymer concentrations. Figure 5 illustrates the effects of the triblock copolymer concentrations on LCST and CP values for PEG₄₃-*b*-PNIPAM₈₂-*b*-PCL₈₇ samples. As the polymer concentrations decrease from 1.0 to 0.1 mg/mL, LCST values increase from 33 to 36 °C for PEG₄₃-*b*-PNIPAM₈₂-*b*-PCL₈₇. On the other hand, upon decreasing the polymer concentrations from 1.0 to 0.1 mg/mL, CP values increase from 35 to 40 °C for PEG₄₃-*b*-PNIPAM₈₂-*b*-PCL₈₇. It is found that the present micelles are very stable and can keep suspending in water at temperatures much higher than the LCST, which is ascribed to the hydrophilic PEG block.

To obtain the triblock copolymer micelles, the triblock copolymer was dissolved in THF, and 8-fold of water was added into the solution drop by drop. The solution was dialyzed against double-distilled water for 2 days to remove THF.^{44,45} The structure and dimension of the micelles were studied by direct observations with TEM. Figure 6 shows TEM images of self-assembly of PEG₄₃-*b*-PNIPAM₈₂-*b*-PCL₈₇ in aqueous solution. The micelles are predicted to have a core-shell-corona structure, where the insoluble PCL block forms the core, the soluble PNIPAM block forms the shell, and the PEG block forms the corona of the resultant micelles. Usually, the identification of the core layer, shell layer, and corona layer of core-shell-corona micelles is very difficult or complex. TEM and atomic force microscopy (AFM) measurements are possibly the most popular ways to identify a core-shell-corona micelle. However, a

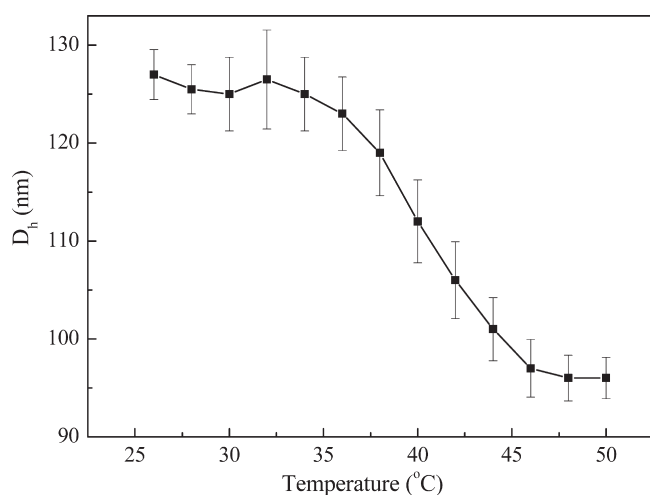


Figure 7. Temperature dependence of the hydrodynamic diameter D_h of the core–shell–corona micelles formed in water with copolymer concentration at 0.050 mg/mL.

core–shell–corona micelle is usually observed to be a sphere by TEM or AFM, which is just like a core–shell one. On the TEM images (Figure 6), we can find that the diameter of the spherical micelles from the self-assembled PEG₄₃-*b*-PNIPAM₈₂-*b*-PCL₈₇ triblock copolymers in water varied from about 90 to 110 nm.

The hydrodynamic diameter (D_h) was determined as a function of temperature with copolymer concentration at 0.050 mg/mL at a 90° scattering angle. Clearly, the hydrodynamic diameter of the core–shell–corona micelles almost keeps a constant of about 125 nm at temperature below 34 °C (Figure 7). When the temperature was further increased, the hydrodynamic diameter decreases gradually until to a smaller constant of about 95 nm at 50 °C. The decrease in size with increased temperature is explained by the PNIPAM chains transforming from a coil to a globular conformation.⁴⁶ This conformational change results in the expulsion of water due to the increased hydrophobicity of the PNIPAM corona chains, and the PNIPAM chains gradually collapse on the PCL core of the core–shell–corona micelles, which decreases the hydrodynamic diameter of the resultant micelles. Herein, the LCST of the shell-forming block is about 34 °C, which is little higher than that of homopolymer PNIPAM.^{47,48} The possible reason is that the hydrophilic PEG block enhances the solubility of the PNIPAM. It must be noted that the values of the hydrodynamic diameter of the core–shell–corona micelles measured by DLS are larger than those observed by TEM. This is because the core–shell–corona micelles are water-swollen due to the soluble PEG and PNIPAM blocks, whereas TEM observation shows the diameter of the dried aggregates.

CONCLUSION

In this research, it was confirmed that ATRP is a particularly suitable polymerization technique for combination with the click 1,3-dipolar cycloaddition reaction of azides and terminal alkynes, as it permits one to introduce both alkyne and azide functionalities into a polymer chain. The particular combination of ATRP, ROP, and click chemistry is a promising strategy to synthesize functional telechelics due to efficient postpolymerization modification afforded by Cu(I)-catalyzed azide–alkyne coupling. Characteristics of controlled polymerization were

observed, and the resulting azido-functionalized polymers were reacted with alkyne functional PCL to obtain the block polymers. The reaction products were confirmed by FTIR, GPC, and ¹H NMR spectroscopy. Temperature-dependent turbidimetry was then employed to determine CP values of PEG₄₃-*b*-PNIPAM₈₂-*b*-PCL₈₇ micelles in aqueous solutions, and it depends on the block copolymer concentration, which increases from 35 to 40 °C when the copolymer concentration decreases from 1.0 to 0.1 mg/mL. The behavior of the triblock copolymer in aqueous solution was also studied by DLS and TEM. The ability to synthesize block copolymers that are thermoresponsive and water-soluble will be of great benefit for broader applications in drug delivery, bioengineering, and nanotechnology.

AUTHOR INFORMATION

Corresponding Author

*Tel.: +86 931 8912387. Fax: +86 931 8912582. E-mail: mzliu@lzu.edu.cn, chenjc2010@lzu.edu.cn.

ACKNOWLEDGMENT

The financial support of the Special Doctoral Program Funds of the Education of China (Grant No. 20090211110004) and Gansu Province Project of Science and Technologies (Grant No. 0804WCGA130) is gratefully acknowledged.

REFERENCES

- (1) Kataoka, K.; Harada, A.; Nagasaki, Y. *Adv. Drug Delivery Rev.* **2001**, *47*, 113–131.
- (2) Wei, H.; Cheng, S. X.; Zhang, X. Z.; Zhuo, R. X. *Prog. Polym. Sci.* **2009**, *34*, 893–910.
- (3) Qiao, P.; Niu, Q. S.; Wang, Z. B.; Cao, D. P. *Chem. Eng. J.* **2010**, *159*, 257–263.
- (4) Cheng, Z. P.; Zhu, X. L.; Kang, E. T.; Neoh, K. G. *Langmuir* **2005**, *21*, 7180–7185.
- (5) Qin, J. L.; Jiang, X. B.; Gao, L.; Chen, Y. M.; Xi, F. *Macromolecules* **2010**, *43*, 8094–8100.
- (6) Li, G. Y.; Shi, L. Q.; An, Y. L.; Zhang, W. Q.; Ma, R. J. *Polymer* **2006**, *47*, 4581–4587.
- (7) Li, J.; He, W. D.; Sun, X. L. *J. Polym. Sci., Part A: Polym. Chem.* **2007**, *45*, 5156–5163.
- (8) Lei, L.; Gohy, J. F.; Willet, N.; Zhang, J. X.; Varshney, S.; Jérôme, R. *Macromolecules* **2004**, *37*, 1089–1094.
- (9) Yu, G.; Eisenberg, A. *Macromolecules* **1998**, *31*, 5546–5549.
- (10) Zhang, W. Q.; Jiang, X. W.; He, Z. P.; Xiong, D.; Zheng, P. W.; An, Y. L.; Shi, L. Q. *Polymer* **2006**, *47*, 8203–8209.
- (11) Matmour, R.; More, A. S.; Wadgaonkar, P.; Gnanou, Y. *J. Am. Chem. Soc.* **2006**, *128*, 8158–8159.
- (12) Wetering, K. V. D.; Brochon, C.; Ngov, C.; Hadzioannou, G. *Macromolecules* **2006**, *39*, 4289–4297.
- (13) Kolb, H. C.; Finn, M. G.; Sharpless, K. B. *Angew. Chem., Int. Ed.* **2001**, *40*, 2004–2021.
- (14) He, X. H.; Liang, L. Y.; Xie, M. R.; Zhang, Y. Q.; Lin, S. L.; Yan, D. Y. *Macromol. Chem. Phys.* **2007**, *208*, 1797–1802.
- (15) Ranjan, R.; Brittain, W. J. *Macromolecules* **2007**, *40*, 6217–6223.
- (16) Wang, Y. P.; Chen, J. C.; Xiang, J. M.; Li, H. J.; Shen, Y. Q.; Gao, X. H. *React. Funct. Polym.* **2009**, *69*, 393–399.
- (17) Mahouche-Chergui, S.; Gam-Derouich, S.; Mangeney, C.; Chehimi, M. M. *Chem. Soc. Rev.* **2011**, *40*, 4143–4166.
- (18) Mahouche-Chergui, S.; Ledebt, A.; Mammeri, F.; Herbst, F.; Carbonnier, B.; Ben Romdhane, H.; Delamar, M.; Chehimi, M. M. *Langmuir* **2010**, *26*, 16115–16121.
- (19) Xu, J.; Ye, J.; Liu, S. Y. *Macromolecules* **2007**, *40*, 9103–9110.

- (20) Zhao, C. Z.; Wu, D. X.; Lian, X. M.; Zhang, Y.; Song, X. H.; Zhao, H. Y. *J. Phys. Chem. B* **2010**, *114*, 6300–6308.
- (21) Golas, P. L.; Matyjaszewski, K. *QSAR Comb. Sci.* **2007**, *11*–12, 1116–1134.
- (22) Siegwart, D. J.; Oh, J. K.; Matyjaszewski, K. *Prog. Polym. Sci.* **2012**, *37*, 18–37.
- (23) Couet, F.; Rajan, N.; Mantovani, D. *Macromol. Biosci.* **2007**, *7*, 701–718.
- (24) Nair, L. S.; Laurencin, C. T. *Prog. Polym. Sci.* **2007**, *32*, 762–798.
- (25) Feng, X. S.; Taton, D.; Ibarboure, E.; Chaikof, E. L.; Gnanou, Y. *J. Am. Chem. Soc.* **2008**, *130*, 11662–11676.
- (26) Feng, X. S.; Taton, D.; Borsali, R.; Chaikof, E. L.; Gnanou, Y. *J. Am. Chem. Soc.* **2006**, *128*, 11551–11562.
- (27) Nuopponen, M.; Ojala, J.; Tenhu, H. *Polymer* **2004**, *45*, 3643–3650.
- (28) Manickam, D. S.; Oupicky, D. *Bioconjugate Chem.* **2006**, *17*, 1395–1403.
- (29) Moustafine, R. I.; Salachova, A. R.; Frolova, E. S.; Kemenova, V. A.; Van den Mooter, G. *Drug Dev. Ind. Pharm.* **2009**, *35*, 1439–1451.
- (30) Wiltshire, J. T.; Qiao, G. G. *Macromolecules* **2006**, *39*, 9018–9027.
- (31) Kricheldorf, H. R.; Kreiser-Saunders, I. *Macromolecules* **2000**, *33*, 702–709.
- (32) Ciampolini, M.; Nardi, N. *Inorg. Chem.* **1966**, *5*, 41–44.
- (33) Yuan, Y. Y.; Wang, Y. C.; Du, J. Z.; Wang, J. *Macromolecules* **2008**, *41*, 8620–8625.
- (34) Zhang, W. Q.; Shi, L. Q.; Wu, K.; An, Y. L. *Macromolecules* **2005**, *38*, 5743–5747.
- (35) Pan, Y. V.; Wesley, R. A.; Luginbuhl, R.; Denton, D. D.; Ratner, B. D. *Biomacromolecules* **2001**, *2*, 32–36.
- (36) Xia, Y.; Yin, X.; Burke, N. A. D.; Stöver, H. D. H. *Macromolecules* **2005**, *38*, 5937–5943.
- (37) Queffelec, J.; Gaynor, S. G.; Matyjaszewski, K. *Macromolecules* **2000**, *33*, 8629–8639.
- (38) Tu, C. W.; Kuo, S. W.; Chang, F. C. *Polymer* **2009**, *50*, 2958–2966.
- (39) Lutz, J. F.; Brner, H. G.; Weichenhan, K. *Macromolecules* **2006**, *39*, 6376–6383.
- (40) Bao, H. Q.; Li, L.; Gan, L. H.; Ping, Y.; Li, J.; Ravi, P. *Macromolecules* **2010**, *43*, 5679–5687.
- (41) Zhang, W. A.; Müller, A. H. E. *Macromolecules* **2010**, *43*, 3148–3152.
- (42) Quémener, D.; Davis, T. P.; Barner-Kowollik, C.; Stenzel, M. H. *Chem. Commun.* **2006**, 5051–5053.
- (43) Qiu, X. P.; Tanaka, F.; Winnik, F. M. *Macromolecules* **2007**, *40*, 7069–7071.
- (44) Bae, Y.; Fukushima, S.; Harada, A.; Kataoka, K. *Angew. Chem., Int. Ed.* **2003**, *42*, 4640–4643.
- (45) Jule, E.; Nagasaki, Y.; Kataoka, K. *Langmuir* **2002**, *18*, 10334–10339.
- (46) Wang, X.; Wu, C. *Macromolecules* **1999**, *32*, 4299–4301.
- (47) Wu, C.; Qiu, X. *Phys. Rev. Lett.* **1998**, *80*, 620–622.
- (48) Virtanen, J.; Holappa, S.; Lemmetyinen, H.; Tenhu, H. *Macromolecules* **2002**, *35*, 4763–4769.